RESEARCH ARTICLE

OPTICAL CONSTANTS AND DISPERSION PARAMETERS of $BaSr_{0.6}Fe_{0.4}TiO_3$

[1]Reenu Jacob and [2]Jayakumari Isac*

[1]Department of Physics, CMS College, Kottayam
[2]Centre for Condensed Matter, Department of Physics, CMS College, Kottayam, India

ABSTRACT

A new lead free nano perosvkite **$BaSr_{0.6}Fe_{0.4}TiO_3$** was synthesized through ball milling solid state reaction technique and UV-VIS analysis of the sample was carried out. Tunable band gaps can be obtained by varying annealing temperatures. The optical constants of refractive index, extinction coefficient, normal-incidence reflectivity, and absorption coefficient showed systematic variation with temperature. The dispersion of refractive index was analyzed by the Wemple- Di Domenico single-oscillator model.

INTRODUCTION

Barium strontium titanate (BST) with high dielectric constant ( ) have gained much attention as materials for environmental applications (dielectric for capacitors, actuators, etc.). This perovskite-based ferroelectric, is one of the most studied, exhibiting normal first- order phase transition behaviour. It was previously reported that in Fe-doped $(Ba_{1-x}Sr_x)TiO_3$ micro-structural and dielectric properties were modified by controlling the Fe concentration with fixed Sr concentrations [1-9]. Earlier reports on the dielectric properties of $Ba_xSr_{1-x}TiO_3$ ceramic solid solutions have shown that the compositions exhibited normal ferroelectric behaviour and the loss factor in these materials is reduced with the addition of a proper substitute or doping. Few authors have reported the substitution of Fe in BST where Fe_{3+} ion substitutes Ti_{4+} in BST which reduces the dissipation factor due to domain wall motion [10-12].

Measuring the band gap is an important factor determining the electrical conductivity in nano material industries. The band gap energy of insulators is large (> 4eV), but lower for semiconductors (< 3eV). In solid state physics a band gap, is an energy range in an ideal solid where no electron states can exist. This is equivalent to the energy required to free an outer shell electron from its orbit about the nucleus to become a mobile charge carrier, able to move freely within the solid material [13].

In the present work the authors describes the optical behaviour of **$BaSr_{0.6}Fe_{0.4}TiO_3$**, a lead free material since they are now at the top as ferroelectric and piezoelectric materials. The energy band gap values of sample are analyzed for different temperatures and they are fundamentally important to the design of practical devices [14]. The band gap energy values obtained using Tauc plot shows a direct relation with temperature. The Urbach energy of the sample is also studied. The optical constants of refractive index, extinction coefficient, and absorption coefficient showed a systematic variation with temperature. The dispersion of refractive index is analyzed by the Wemple-DiDomenico single-oscillator model and such optical behaviour is rarely reported.

Experimental

The new ceramic sample **$BaSr_{0.6}Fe_{0.4}TiO_3$** was prepared by the solid state reaction technique using a high-energy ball milling process through mechanically assisted synthesis. For preparing sample, the reagent grade chemicals of high purity Barium Carbonate, Strontium Carbonate, Ferric Oxide and Titanium dioxide powders were used as the raw materials and weighed according to their molecular formula.

The sample was ball milled for three weeks with suitable zirconium balls to insure homogeneity and milling. Then it was attrition milled for three hours. After milling the material was calcined at four different temperatures, 30˚C, 550˚C, 850˚C & 950˚C in a special furnace with oxygen flow arrangements. High temperature is needed for metal oxide phase transformation [15].

UV-VIS. Analysis

The UV analysis can be thought as a good quality check for the optical behaviour of the ceramic materials. The sample obtained after calcination at different temperatures was subjected to UV-VIS-Near IR analysis (Fig.1) using Varian, Cary 5000 Spectrophotometer over a spectral range of 175-3300nm with an accuracy of ±0.1nm (UV-Vis.). This type of sample has high mechanical hardness, high thermal conductivity, large dielectric constant, and high resistance to harsh environment. UV-Visible spectrum give information about the excitonic and inter transition of nano materials [16]. Figure.1 shows the UV-VIS behaviour of the sample **$BaSr_{0.6}Fe_{0.4}TiO_3$** at different temperatures 30[0]C, 550[0]C, 850[0]C & 950[0]C.

The average transmittance in the visible part of the spectra (300-800nm) is about (80-90) %. The diffuse reflectance spectra were translated into the absorption spectra by the

* Corresponding author: **Jayakumari Isac**
Centre for Condensed Matter, Department of Physics, CMS College, Kottayam, India

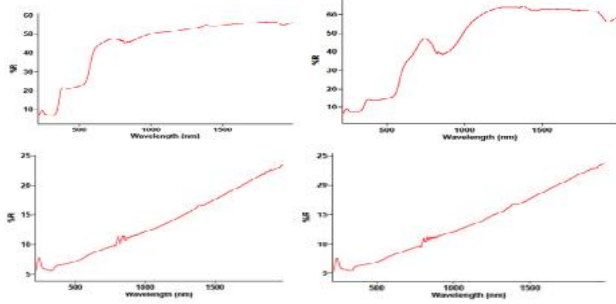Kubelka-Munk method. Kubelka-Munk's equation is described as follows:

Figure1 UV-VIS spectrum of *BaSr$_{0.6}$Fe$_{0.4}$TiO$_3$* at different temperatures 30^{0}C, 550^{0}C, 850^{0}C & 950^{0}C.

=(1-R)2/2R -(1), where is the absorption coefficient and R the reflectivity at a particular wavelength [17].

Band gap energy

The band gap energy can be determined using the Tauc relation. According to the Tauc relation, the absorption coefficient for a material is given by = A(h - Eg)^n-- (2), Where Eg the band gap, constant A is different for different transitions, (hv) is energy of photon in eV and n denotes the nature of the sample transition[18].The TAUC plot of a sample defines the optical band gap as the region A in fig.2.
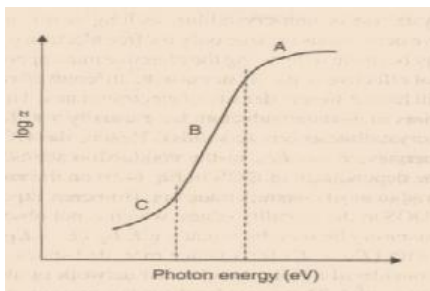

Fig.2 optical band gap energy variation with absorption

The tauc plot of the sample at different temperatures are given in Fig 4(a).

The extinction coefficient and the absorption coefficient are related as (E) =4 / (k(E))—(3).

The absorption coefficient at the photon energy below the optical gap (tail absorption) depends exponentially on the photon energy: (v) ~ exp (v/E$_u$) --(4) where E$_u$ is called Urbach energy.The region B in the fig.2 represents the Urbach energy. The absorption edge called the Urbach energy, depends on temperature, thermal vibrations in the lattice, induced disorder, static disorder, strong ionic bonds and on average photon energies [19]. The edge arises due to a radiative recombination between trapped electrons and trapped holes in tail and gap states as shown in Fig.2, and is dependent on the degree of structural and thermal disorder [20].

The natural logarithm of the absorption coefficient, ( ), was plotted as a function of the photon energy, h (Fig.3). The value of Eu was calculated by taking the reciprocal of the slopes of the linear portion in the lower photon energy region of curves.

The measurement of temperature-dependent Urbach tails distinguishes a temperature-dependent tail and a temperature-independent part, which mainly are due to intrinsic defects. The latter can be controlled by improving the crystal growth and the

purity of the ingradients. The temperature-dependent part of the Urbach tail, is purely of intrinsic reasons [21].

In addition, optical absorption by defects also appears at energy lower than optical gap (region C of fig.2). This region is related to the structural properties of materials[22].

Refractive Index Variation and Dispersion

Refractive index with wavelength dependence was also studied. The refractive index values show a linear decrease with the increase in wavelength, Fig.5 shows the variation of the dispersion curve with annealing temperatures. The refractive index values showed a linear decrease with the increase in wavelength when plotted with refractive index along the Y-axis & wavelength along the X axis. But refractive index value shows a slight increase with increasing annealing temperature and attains a fixed value after a particular wavelength.

The dispersion of refractive index below the interband absorption edge is analyzed using the Wemple-DiDomenico (W-D) model [23]. In the W-D model, the refractive index *n* can be written as $n^2 - 1 = E_d E_0 / (E_d^2 - E^2)$ -- (5),

where *E* is the photon energy, *E$_o$* is the oscillator energy, and *E*d is the dispersion energy. Wemple and DiDomenico reported that the dispersion energy may depend upon the charge distribution within each unit cell, and that it would be closely related to chemical bonding [23]. The oscillator energy *E$_o$* and dispersion energy *E$_d$* are obtained from the slope $(E_o E_d)^{-1}$ and intercept *Eo/E*d on the vertical axis of the straight line portion of $(n^2-1)-1$ versus E^2 plot. The static refractive index *n*(0) at zero photon energy is evaluated from Equation (5), i.e. $n^2(0)=1+E_d/E_o$—(6) [24].

RESULTS AND DISCUSSION

The optical analysis of the ceramic material prepared by solid state reaction technique and treated at different temperatures is successfully done using UV-Vis Spectro photometer. UV-VIS analysis, clearly confirms that band gap energy of the nano ceramic increases first as the temperature is increased but shows a sharp decrease at high temperatures.

The calculated values of the band gap energy of the sample of at different values of temperature is given in the table -1. The sample *BaSr$_{0.6}$Fe$_{0.4}$TiO$_3$* at temperatures 30 C, 550 C, 850 C & 950 C is analysed and studied. Here the direct allowed transitions are considered. The Tauc plot is plotted with hv along the X-axis and (hv)^2 along the Y-axis. The band gap at a particular temperature is found by extrapolating the X axis. The Tauc plot for temperatures 850 C &950 C are given below in Fig.4(a).
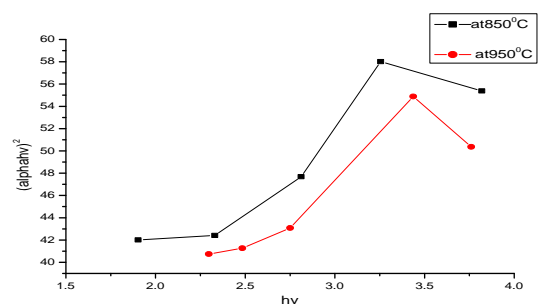

Fig.4 a. The Tauc plot of *BaSr$_{0.6}$Fe$_{0.4}$TiO$_3$* for temperatures 850 C &950 C

The band gap energy values of $BaSr_{0.6}Fe_{0.4}TiO_3$ at different temperatures calculated are listed in the table.1 given below.

Table1 Band gap energy values of $BaSr_{0.6}Fe_{0.4}TiO_3$ at different temperatures

Temperature	Band gap energy in eV
30 C	3.99
550 C	4.58
850 C	3.819
950 C	3.76

From the results it is confirmed that band gap energy rises and slows down with the increase in temperature(fig.4(b). The energy levels are dependent on the degree of structural order–disorder in the lattice. The band gap increases with the crystallite size but decreases as the perosvkite phase is formed which proves the quantum confinement also decreasing its dislocation density. The decrease in band gap energy shows that the sample tends to be more conducting as the temperature is increased.
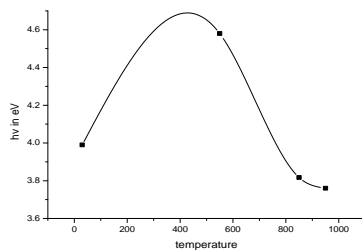

Fig.4 b. Band gap energy with temperature *of* $BaSr_{0.6}Fe_{0.4}TiO_3$

Tauc plot data well confirms that the band gap energy of the sample increases slightly when the temperature is increased. As the temperature is increased the crystallite size also increases which shows an increase in band gap energy[13]. The energy levels are dependent on the degree of structural order–disorder in the lattice. Therefore, the increase of structural organization in nano ceramic leads to a reduction of the intermediaty energy levels and consequently increases the Eg values. But the band gap decreases sharply at high temperature with increase in the crystallite size[15] which very well proves the quantum confinement. This result proves that as the material attains its crystalline phase, the material becomes more conducting and hence the band gap energy falls.

Urbach energy is calculated by plotting the natural logarithm of the absorption coefficient with the energy in eV. This value is found to be lower than the band gap energy and hence Sumi-Toyozawa (ST) model theory can be well applied to this material.
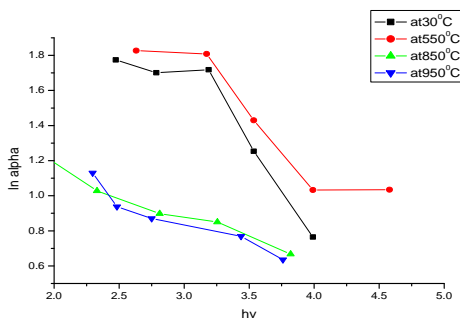

Fig.3 Aabsorption variation with photon energy of $BaSr_{0.6}Fe_{0.4}TiO_3$

The refractive index of the sample at different values of temperature was also studied. Analysis clearly shows that refractive index of the sample decreases as the wavelength increases (varies from 2.27 to 1.76) and attains a definite value

at all temperatures. This linear variation of the refractive index with the wavelength is due to dispersion of light energy at the different interstitial layers. The refractive index also shows a linear relation with the photon energy (fig.5a&b). The refractive index of perovskites is known to be proportional to their electronic polarization per unit volume which is inversely proportional to distance between atomic planes. This result can also be explained by an increase in crystallite size. The increase in refractive index is due to crystallization of the perovskite phase.
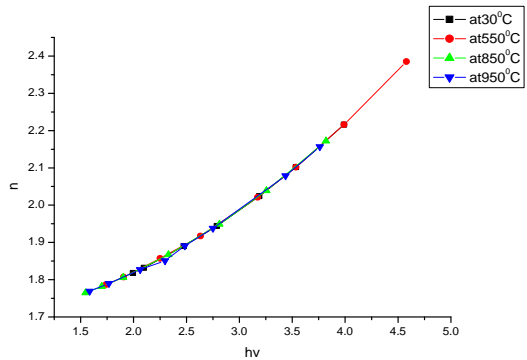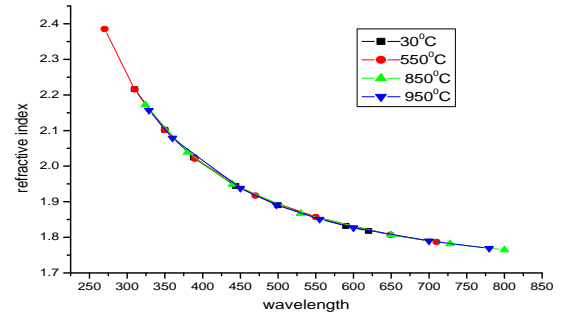

Fig.5 (a & b) Variation of Refractive index **(n)** with wavelength and photon energy for different temperatures($BaSr_{0.6}Fe_{0.4}TiO_3$)

Dispersion Energy

The dispersion energy of the sample is calculated using the Wemple-DiDomenico (WD)model. Results are plotted graphically in (Fig.6).
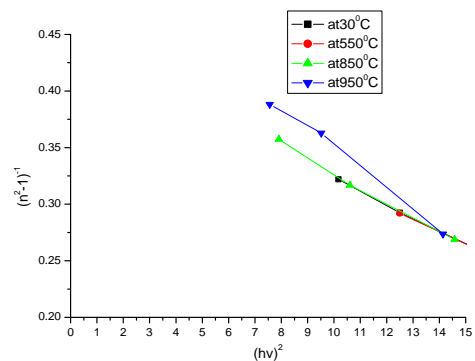

Fig.6 $(n^2-1)^{-1}$ versus $(hv)^2$ curve

The data of the dispersion of the refractive index (n) were evaluated according to the single oscillator model proposed by wimple and DiDomenico as, $n^2 = 1 + (E_d E_0)/(E_0^2 - hv^2)$ ---- (7).

where E_o is the oscillator energy and E_d is the oscillator strength or dispersion energy.

Plotting of $(n^2-1)^{-1}$ against $(hv)^2$ allows to determine, the oscillator parameters, by fitting a linear function to the smaller energy data, E_o and E_d can be determined from the intercept,

(E_o/E_d) and the slope $(1/E_oE_d)$. E_o is considered as an average energy gap to, it varies in proportion to the Tauc gap $E_o \sim 2E_g$.

The oscillator model can be also written as $n^2-1=S_0 \ _0^2/[1-(\ _o / \ )^2]$ --- (8) where is the wavelength of the incident radiation , S_o is the average oscillator strength and $_o$ is an average oscillator wavelength.

The curves of $(n^2 – 1)^{-1}$ against $(1/ \ ^2)$ (Fig.7) are fitted into straight lines following the sell Meier's dispersion formula . The value of S_o and $(\ _o)$ are estimated from the slope $(1/So)$ and the infinite wavelength intercept $(1/S_0 \ _o)^2$. The optical parameters of the sample were calculated and listed in the table.2 given below.

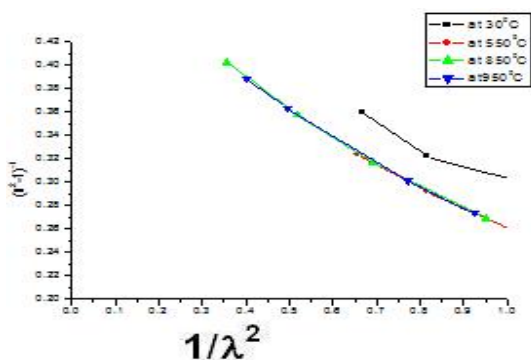**Fig.7**-$(n^2-1)^{-1}$ versus $1/ \ ^2$ curve

Table 2 The optical parameters of ($BaSr_{0.6}Fe_{0.4}TiO_3$) calculated

sample	$E_g(eV)$	$E_O(eV)$	$E_d(eV)$
at 850 C	3.819	6.635	12.66
At 950 C	3.76	5.125	11.38

From the analysis it is clear that as the temperature is increased band gap energy decreases or E_0 decreases respectively. The dispersion energy also shows a decline as the temperature rises and the sample attains its perosvkite phase. The curves with straight line graphs confirms the sell Meier's dispersion formula. Further the mechano chemical process has an advantage due to low-costs and widely available materials, leading to a simplified process.

CONCLUSION

The optical properties of the new nano ceramic material $BaSr_{0.6}Fe_{0.4}TiO_3$ can be taken as a better candidate for UV_VIS shielding applications. A sound understanding of the band gap variations of the sample with different temperatures are noted The UV emission peak shifts significantly to higher wavelengths with increasing annealing temperatures. It is confirmed that tunable band gaps are obtained by varying annealing temperatures. The increase in the band gap energy increases the dielectric properties of the material. Results of optical measurements show that absorbance and reflectance increases with temperature.

The dispersion energy also decreases as the sample attains its perosvkite phase. This was analysed using the Wemple-DiDomenico single-oscillator model. As the band gap energy falls at high temperature the material becomes more conducting and hence $BaSr_{0.6}Fe_{0.4}TiO_3$ materials will definitely prove as a future substitute for the engineering of new generation capacitors.

References

1. A. Sundaresan and C. N. R. Rao, "Ferromagnetism as a Universal Feature of Inorganic Nanoparticles," *Nano Today*, Vol. 4, No. 1, 2009, pp. 96-106. doi:10.1016/j.nantod.2008.10.002

2. C. Mao, X. Dong, T. Zeng, H. Chen, F. Cao, Ceramics International, Vol. 34, 2008, pp. 45.

3. Choudhury *et al. International Nano Letters* **2013** **3**:25 doi:10.1186/2228-5326-3-25 licensee Springer

4. Dennis P. Shay -Development And Characterization Of High Temperature, High Energy Density Dielectric Materials To Establish Routes Towards Power Electronics Capacitive Devices- The Pennsylvania State University The Graduate School Department of Materials Science and Engineering May2014.
   Electronic Materials and Devices Laboratory, Department of Railroad Drive and Control, Dongyang University, Yeongju 750-711, Korea pISSN: 1229-7607 eISSN: 2092-7592.

5. F. Lin and W. Shi, "Effect of Sr Concentration on Microstructure and Magnetic Properties of (Ba1–xSrx) (Ti0.3Fe0.7) O3 Ceramics," *Journal of Magnetism and Magnetic Ma- terials*, Vol. 322, No. 14, 2010, pp. 2081-2085. doi:10.1016/j.jmmm.2010.03.004

6. H. I. Hsing, C. S. Hsib, C. C. Huang and S. L. Fu, "Low Temperature Sintering and Dielectric Properties of BaTiO3 with Glass Addition" *Materials Chemistry and Physics*, Vol. 113, No. 2-3, 2009, pp. 658-663. 10.1016/j.matchemphys.2008.08.033

7. H. Sumi and Y. Toyozawa, J. Phys. Soc. Jpn. 31, 342 (1971).

8. K. Battisha, A. B. Abou Hamad and R. M. Mahani, "Structure and Dielectric Studies of Nano-Composite Fe2O3: BaTiO3 Prepared by Sol-Gel Method," *Physica B*, Vol. 404, No. 16, 2009, pp. 2274-2279. doi:10.1016/j.physb.2009.04.038

9. Keigo Suzuki, And Kazunori Kijima. 2005. Optical Band Gap Of Barium Titanate Nanoparticles Prepared By Rf-Plasma Chemical Vapor Deposition, Japanese Journal of Applied Physics, Vol. 44, No. 4a, 2005, Pp. 2081–2082, The Japan Society of Applied Physics.

10. L. B. Kong, T. S. Zhang, J. Ma and F. Boey, "Progress in Synthesis of Ferroelectric Ceramic Materials Via High-Energy Mechanochemical Technique" *Progress in Materials Science*, Vol. 53, No. 2, 2008, pp. 207-322. doi:10.1016/j.pmatsci.2007.05.001

11. M. Letz,1 A. Gottwald,2 M. Richter,2 V. Liberman,3 and L. Parthier4 1*Schott AG,* Temperature-dependent Urbach tail measurements of lutetium aluminum garnet single crystal -*Research and Development, Hattenbergstr. 10, D-55014 Mainz, Germany* 2*Physikalisch-Technische Bundesanstalt (PTB), Abbestr. 2-12, D-10587 Berlin, Germany* 3*Lincoln Laboratory, MIT, 244 Wood St., Lexington, Massachusetts 02420-9108, USA* 4*Schott Lithotec AG, Otto-Schott-Str. 13, D-07745 Jena, Germany-* .- physical review B **81**, 155109 _2010.

12. M. Roscher, T. Schneller, R. Waser, J. Sol-Gel Sci. Tech., Vol. 56, 2010, pp. 236.

13. N. Nepal, J. Li, M. L. Nakarmi, J. Y. Lin, and H. X. Jianga_ Temperature and compositional dependence of the energy band gapof AlGaN alloys *Department of Physics, Kansas State University, Manhattan, Kansas 66506-2601*

14. R. Kavian and A. Saidi, "Sol-Gel Derived BaTiO3 Nano-Powders," *Journal of Alloys and Compounds*, Vol. 468, No. 1-2, 2009, pp. 528-532. doi:10.1016/j.jallcom.2008.01.045

15. Reenu Jacob, Harikrishnan G Nair, Jayakumari Isac- OPTICAL BAND GAP ANALYSIS OF NANO-CRYSTALLINE CERAMIC PbSrCaCuO, Journal of Advances in Physics,2014,ISSN 2347-3487.

16. S. H. Wemple and M. DiDomenico, Jr., Phys. Rev. B 3, 1338 (1971).

17. S. Kugler: Lectures on AmorphousSemiconductors- 4 May 2013 **...** www.slideserve.com/Leo/optical-properties.

18. Tauc, J., Menth, A., 1972 Non Cryst. Solids 569 8

19. Vinila, V.S., Jacob, R., Mony, A., Nair, H.G., Issac, S., Rajan, S., Nair, A.S. and Isac, J. (2014) XRD Studies on Nano Crystalline Ceramic Superconductor PbSrCaCuO at Different Treating Temperatures. *Crystal Structure Theory and Applications*, **3**, 1-9. http://dx.doi.org/10.4236/csta.2014.

20. W. Li, Z. Xu, R. Chu, P. Fu, J. Hao, *Journal of Alloys and Compounds*, Vol. 482, 2009, p. 137.

21. Willander1, O. Nur1, M. Q. Israr1, A. B. Abou Hamad2, F. G. El Desouky 2, M. A. Salem2, I. K. Battisha2* Determination of A.C. Conductivity of Nano-Composite Perovskite Ba(1–x–y)Sr(x)TiFe(y)O3 Prepared by the Sol-Gel TechniqueM-*Journal of Crystallization Process and Technology*, 2012, 2, 1-11 http://dx.doi.org/10.4236/jcpt.2012.21001 Published Online January 2012 (http://www.SciRP.org/journal/jcpt)

22. Wug-Dong Park-- Optical Constants and Dispersion Parameters of CdS Thin Film Prepared by Chemical Bath Deposition

23. X. Wei, G. Xu, Z. Ren, Y. Wang, G. Shen and G. Han, "Size-Controlled Synthesis of BaTiO3 Nanocrystals via a Hydrothermal Route," *Materials Letters*, Vol. 62, No. 21-22, 2008, pp. 3666-3669.

24. Z. Shao, G. Xiong, J. Tong, H. Dong, W. Yang, "Ba Effect in Doped Sr(Co0.8Fe0.2)O3- on the Phase Structure and Oxygen Permeation Properties of the Dense Ceramic Membranes," *Separation and Purification Technology*, Vol. 25, No. 1-3, 2001, pp. 419-429. doi:10.1016/S1383-5866(01)00071-5

****